CRYSTALLIZATION OF COMPLEXES

Acta Cryst. (1994). D**50**, 512–520

Crystallographic Studies on p21$^{H\text{-}ras}$ Using the Synchrotron Laue Method: Improvement of Crystal Quality and Monitoring of the GTPase Reaction at Different Time Points

BY AXEL J. SCHEIDIG, ANTONIETA SANCHEZ-LLORENTE AND ALFRED LAUTWEIN

Max-Planck-Institut für medizinische Forschung, Abteilung Biophysik, Jahnstrasse 29, 69028 *Heidelberg, Germany*

EMIL F. PAI

Department of Biochemistry and Molecular and Medical Genetics, University of Toronto, Medical Sciences Building, Ontario M5S 1*A*8, *Canada*

JOHN E. T. CORRIE AND GORDON P. REID

National Institute for Medical Research, Mill Hill, London NW7 1*AA, England*

AND ALFRED WITTINGHOFER AND ROGER S. GOODY*

Max-Planck-Institut für molekulare Physiologie, Rheinlanddamm 201, 44026 *Dortmund, Germany*

(*Received* 10 *September* 1993; *accepted* 22 *December* 1993)

Abstract

The parameters affecting the crystal quality of complexes between p21$^{H\text{-}ras}$ and caged GTP have been investigated. The use of pure diastereomers of caged GTP complexed to the more stable p21(G12P)′ mutant of p21 and the addition of *n*-octyl-β-D-glucopyranoside improved the reproducibility and decreased the mosaicity of the crystals significantly. Furthermore, the crystallization technique was changed from the batch method to the sitting-drop technique. With the availability of a larger yield of well ordered crystals, it was possible to extend the time-resolved crystallographic investigations on p21$^{H\text{-}ras}$. A structure of p21(G12P)′:GTP could be obtained 2 min after photolytic removal of the cage group and led to the identification of a previously unidentified conformation for the so-called catalytically active loop *L*4. The refinement of five data sets collected within 2 min at different times (2–4, 11–13, 20–22, 30–32 and 90–92 min) after the initiation of the intrinsic GTPase reaction of the protein indicates that the synchrotron Laue method can be used to detect small structural changes and alternative conformations, but is presently limited in the analysis of larger rearrangements since these produce diffuse and broken electron density.

* Author to whom all correspondence should be addressed

Abbreviations

p21c′, truncated p21$^{H\text{-}ras}$ (residues 1–166); p21(G12P)′, truncated p21$^{H\text{-}ras}$ with the mutation G12P; SA, simulated annealing; r.m.s., root mean square.

Introduction

X-ray crystallography and multidimensional NMR techniques are revealing more and more three-dimensional protein structures. These structures are the basis for rational structure-based work on and with proteins. Due to the long data-acquisition times, these methods are limited to long-lived structures. Since protein reactions are dynamic processes, time-resolved techniques are needed to investigate them. The revival of the Laue method [stationary crystal, polychromatic X-ray diffraction analysis (Friedrich, Knipping & Laue, 1912; Amoros, Buerger & Amoros, 1975)] for protein and virus crystallography in the past decade has resulted in a number of new structures being solved (for reviews see, Moffat, 1989; Helliwell *et al.*, 1989; Hajdu & Johnson, 1990; Hajdu & Andersson, 1993). The main advantages of this synchrotron technique are the high efficiency for recording X-ray diffraction data and the enormous reduction of the acquisition time. Therefore, using this technique, it should be possible

to study reactions in crystals which could improve our understanding of enzyme reactions.

$p21^{H\text{-}ras}$ was one of the first proteins for which the structure of an unstable complex with a substrate (GTP) was determined by time-resolved Laue crystallography (Schlichting *et al.*, 1990). The human proto-oncogene product $p21^{H\text{-}ras}$ is a small (apparent molecular weight = 21 kDa) guanine nucleotide binding protein which is believed to function as a molecular switch in signalling events of cell growth and differentation (for reviews, see Barbacid, 1987; McCormick, 1989). The switch is 'on' if GTP is bound and 'off' in the GDP-bound state. p21 is inactivated in the sense of signal transduction by the hydrolysis of GTP to GDP, which is performed either by the protein itself or in an accelerated manner by interacting with effector proteins called GAP (GTPase activating protein) such as p120-GAP or NF1-GAP (Bollag & McCormick, 1991). The question of how this on–off cycle works at the molecular level has aroused considerable interest. The crystal structures of p21 complexed with non-hydrolyzable GTP analogs and with GDP have different conformations (Pai *et al.*, 1990; Milburn *et al.*, 1990; Jurnak, Heffron & Bergmann, 1990). The conformational transition due to the hydrolysis of GTP to GDP seems to be the key to the mechanism of all guanine nucleotide binding proteins.

These conformational changes of p21 during the intrinsic GTPase reaction are the focus of the time-resolved investigations. The intrinsic GTPase rate of p21 ($T_{1/2}$ = 23 min in solution and $T_{1/2}$ = 40 min in the crystal, both at 293 K) is slow. Fast and uniform reaction initiation throughout the crystal is, therefore, no problem when using photolysis of caged GTP, a biologically inert precursor of GTP. Previous kinetic Laue studies on p21 were hampered by the low quality (high mosaicity) of the p21′:caged-GTP crystals: only two out of 26 crystals of wild-type p21 were ordered enough for data processing. Data sets were collected 4 and 14 min after photolysis, representing the p21′:GTP and a mixed p21′:GTP/p21′:GDP complex, respectively. It was hoped that substituting the racemic mixture of C1-caged(*R*,*S*)-GTP (see Fig. 1) with the pure diastereomers or the use of other cage compounds would improve the crystal quality both in terms of mosaicity and resolution. The demand for high-quality crystals is a serious problem for polychromatic diffraction analysis, since the white-beam method is much more sensitive towards lattice imperfections. A high mosaic spread will cause streaky reflections and any crack will lead to distorted spots or spots with small satellites. Both types of spots make the data processing very difficult or even impossible, but in any case the resulting data are of lower quality. These types of imperfections can have multiple origins, one being the initial crystallization, the others are crystal mounting, triggering and radiation damage. In this paper we present strategies for reducing crystal damage and give a summary of time-resolved crystallographic studies on $p21^{H\text{-}ras}$.

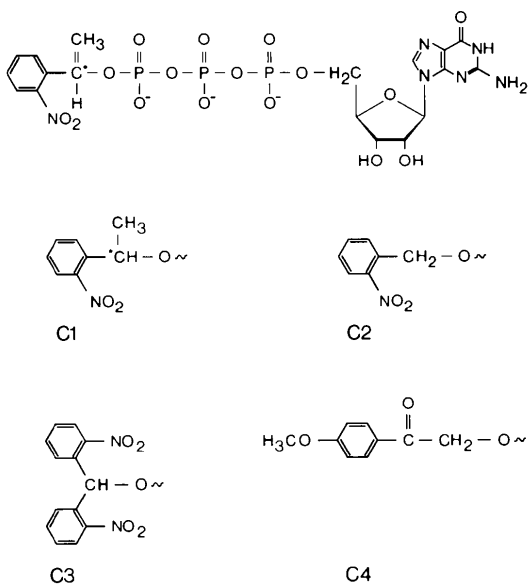

Fig. 1. Structures of the four different cage groups used for caged GTP during the crystallographic studies on $p21^{H\text{-}ras}$. C1: 1-(2-nitrophenyl)ethyl-, the asterisk marks the asymmetric substituted C atom of the cage group; caged (*R*,*S*)-GTP is a mixture of pure caged(*R*)-GTP and pure caged(*S*)-GTP (ratio *ca* 1:1) according to Cahn–Ingold–Prelog nomenclature; C2: 2-nitrobenzyl-; C3: bis(2-nitrophenyl)methyl-; C4: 2-oxo-2-(4-methoxyphenyl)ethyl-.

Experimental

Purification, nucleotide exchange, reaction initiation by flash photolysis and reverse-phase (C18) HPLC analysis of the crystal content and state of the nucleotide bound to p21 were performed as described previously (Schlichting *et al.*, 1989). The protocol for crystallization of the complexes was initially as described for p21c′ complexes with caged(*R*,*S*)-GTP (Schlichting *et al.*, 1989) using Tris–HCl (Sigma) as the buffer system and polyethylene glycol 400 (PEG 400, Serva) as precipitant. Crystals were transferred to 0.7 mm quartz capillaries, mounted completely surrounded by artificial mother liquor and immobilized between two plugs of pipe-cleaner fibres. The setup for flash photolysis was as described by Schlichting *et al.* (1989) using a Xenon flash lamp (Rapp & Güth, 1988). For the analysis of the nucleotide content of the crystals, the reaction was stopped by flash-freezing the crystals in liquid nitrogen immediately after the exposure.

All diffraction data were collected at 293 K on experimental station 9.5 (Brammer *et al.*, 1988) at the Daresbury Synchrotron Radiation Source (SRS), using polychromatic radiation in the wavelength

Table 1. *Data statistics for Laue data reduction*

Structure time point (min)	Complex	Number of orientations	Mean intra-pack *R* factor (%)	Total observations	Unique reflections	Percent of total to 2.8 Å	*R* factor for all data (%)	*R* factor within 0.1 Å (%)
0	p'N	3	4.1	6636	2236	56	9.6	6.0
0	c'N	3	4.0	7098	2067	45	8.8	6.2
2 4	p'*R*	4	4.7	8707	2419	63	11.4	7.4
2 4	p'*S*	4	4.6	8723	2590	65	8.7	5.9
11 13	p'*S*	4	3.4	8642	2400	60	10.3	7.3
20 22	p'*S*	4	4.7	6904	2408	60	10.9	8.6
30–32	p'*S*	4	4.8	8200	2698	67	11.7	8.9
55 57	p'*S*	4	3.9	5670	2011	55	11.6	9.5
90–92	p'*R*	3	5.0	5749	2438	62	26.4	14.5

* Complex p'N = p21(G12P)':caged(*R*,*S*)-GppNHp, c'N = p21c':caged(*R*,*S*)-GppNHp, p'*R* = p21(G12P)':caged(*R*)-GTP, p'*S* = p21(G12P)':caged(*S*)-GTP (p'N, c'N, p'*R* and p'*S* with C1-cage group).

range 0.45–2.6 Å on CEA Reflex 25 film (12.5 × 12.5 cm). To reduce radiation damage 1 mm graphite was introduced in the beam path upstream of the collimator (diameter of the collimator = 0.2 mm). Each film pack consisted of six films (*A–F*) with no interleaved metal foils between the films. Crystals were mounted in the capillaries with arbitrary orientations due to the fixation by cotton fibres. No alignment of the crystals relative to the X-ray beam was attempted. The crystal-to-film distance was 90–96 mm. This was the closest distance possible. The camera was an Arndt/Wonacott rotation camera holding eight standard 5″ × 5″ cassettes allowing rapid film changing. To break the symmetry and obtain more unique data the spindle was set to μ = 15°. The reaction was initiated by flashing ten times within 90 s. Data sets were collected before and 2, 11, 20, 30, 50 and 90 min after photolysis. For each time point a fresh crystal was used. Data sets consist of three or four exposures (0.45 to 0.5 s) taken at random orientations of the crystals differing in 20° in the spindle angle φ. The films were scanned at Daresbury on a Scandig 3 rotating-drum microdensitometer with a 50 μm raster size and a density range of 0–2. The soft limits d_{min}, λ_{min} and λ_{max} were estimated from the gnomonic projections of the Laue patterns (Cruickshank, 1992). The data were reduced using a program suite written at Daresbury (Helliwell *et al.*, 1989). Briefly, data reduction consists of finding and refining the crystal orientation (*GENLAUE*), integration of the intensity of the indexed spots at predicted film positions (*INTLAUE*), scaling and Lorentz–polarization correction of the intensities of the spots measured on films *A–F* within one film pack (*AFSCALE*) and wavelength normalization of these intensities using the intensities of Friedel and symmetry-equivalent reflections observed at different wavelengths and to scale together data from several film packs (*LAUENORM*). During the data reduction spatial overlaps and harmonic overlaps were discarded. The data reduction statistics are given in Table 1.

For all time points the refinement started with the high-resolution model of p21c':GppNHp (Pai *et al.*, 1990). In the starting model the loop regions *L2* (residues 32–37) and *L4* (residues 61–65) as well as the nucleotide and water molecules were removed to yield an unbiased electron-density map. These regions are referred to the flexible parts of the protein. The refinement was carried out with the program *X-PLOR* (Brünger, Kuriyan & Karplus, 1987) using a simulated-annealing protocol as suggested (Brünger, 1988) with an initial temperature of 2000 K followed by positional and grouped *B*-factor refinement. The phase information from the atomic model was used in a way similar to the method of Read (1986) which reduces model bias from the new $(2F_o - F_c)$ electron-density map through calculating the electron-density maps with the coefficients $(2mF_o - DF_c)(\exp i\alpha_c)$. The electron-density maps and models were examined using the program *TOM* (Cambillau, 1989). The refinement statistics are summarized in Table 2.*

Results and discussion

To test the influence of the cage group attached to the GTP, four different cage groups (C1–C4) were investigated (see Fig. 1). Early work with p21 was with the mixture of the diastereomers (ratio *ca* 1:1) of the cage group C1 (Schlichting *et al.*, 1990). The cage group C2 is similar to C1 except there is no asymmetrically substituted C atom. Using C2-caged GTP complexed to p21c' it was possible to get crystals but their size was below 200 μm and they diffracted the monochromatic X-ray beam to not better than 3.0 Å. With the cage group C3 it was possible to get large crystals (longest dimension 900 μm) in complex with p21(G12P)' which diffract

* Atomic coordinates and structure factors have been deposited with the Protein Data Bank, Brookhaven National Laboratory. Free copies may be obtained through The Technical Editor, International Union of Crystallography, 5 Abbey Square, Chester CH1 2HU, England (Supplementary Publication No. SUP 37113).

Table 2. *Model statistics at the end of refinement*

Structure time point (min)	Complex	*R* factor (%)	R.m.s. deviation Bond (Å)	Angle ( )	Occupancy of γ-phosphate group (%)
0	p′N	18.4	0.021	2.81	100
0	c′N	Not refined due to very noisy electron-density map			
2-4	p′*R*	Not refined due to very noisy electron-density map			
2-4	p′*S*	19.3	0.027	5.54	100
11-13	p′*S*	17.2	0.029	5.42	70
20-22	p′*S*	19.1	0.021	2.92	50
30–32	p′*S*	21.3	0.023	2.80	20
55–57	p′*S*	Not refined due to very noisy electron-density map			
90-92	p′*R*	15.4	0.035	5.61	0

the monochromatic X-ray beam to a Bragg spacing of 2.6 Å; in complex with wild-type p21c′ the crystals diffracted to 3.2 Å. The crystals with C1- and C2-caged GTP were isomorphous with p21c′:GppNHp (Pai *et al.*, 1990) whereas the complex of p21(G12P)′ or p21c′ with C3-caged GTP were not (results of structure determination and refinement will be published elsewhere). The cage group C4 could not be used for crystallographic studies as C4-caged GTP was unstable under the crystallization conditions and only protein precipitation could be observed. Therefore, only the original cage group C1 was used for the time-resolved crystallographic studies and all results described below are with C1-caged GTP.

One very critical step affecting the crystal quality is the transfer and the mounting of the crystal in the capillary. For the removal of the reactive 2-nitrosoacetophenone leaving group of the photolysis reaction the crystal has to be surrounded by a solution which is enriched in a thiol-containing compound like dithioerythritol (DTE; McCray & Trentham, 1989). Previously p21′:caged-GTP was crystallized by a batch technique using 10 μl drops (initial concentrations: 20–24 mg ml^{-1} protein, 23–24% PEG 400 and 20 m*M* DTE; Schlichting *et al.*, 1989). If the volume of the mother liquor is too small for the mounting of the crystal, an artificial mother liquor has to be mixed with an estimated PEG concentration. To avoid this problem the crystallization technique was changed from batch with 10 μl drops without reservoir solution to sitting drop (using Cryschem plates) with 20 μl drops equilibrated against 1 ml of a reservoir solution. The crystallization conditions were 27–29%(*w*/*v*) PEG 400 in the drop containing the protein with a concentration of 10–15 mg ml^{-1}. Furthermore, it was found to be advantageous to add 0.01–0.05%(*w*/*v*) *n*-octyl-β-D-glucopyranoside (β-OG) to the drop and to change the pH from 7.6 to 8.0. The reservoir was of the same composition as the drop except that the precipitant concentration was 30–34%(*w*/*v*). Using this new protocol, crystals grew to larger than 500 μm within 2 weeks. The addition of detergent reduced the number of twinned crystals significantly. As artificial mother liquor, the reservoir solution was used, enriched with fresh DTE (Sigma) to a final concentration of 50 m*M*. Large crystals of wild-type p21 (p21c′) and the G12P mutant of p21 [p21(G12P)′] could only be obtained by micro-seeding. The dilution of the seed solution [40%(*w*/*v*) PEG 400] was adjusted so that 1 μl seed solution added to the freshly mixed drop will result in 1–3 large crystals. The seed solution could be stabilized for over a year by flash-freezing in liquid nitrogen and storage at 200 K. Depending on which isomer of caged GTP was complexed with p21, the crystals were hexagonal plates or elongated prisms with longest edge along the crystallographic *c* axis (*S* isomer) or thinner prisms with the shortest edge along the *c* axis (*R* isomer). The crystals of the wild-type and mutant forms of p21 complexed with either the *R* isomer or the *S* isomer of caged GTP are isomorphous to p21c′:GppNHp (Scheidig *et al.*, 1992).

The monochromatic crystal structure determination of p21c′:caged(*R*)-GTP and p21c′:caged(*S*)-GTP revealed that the GTP precursor is bound at the active site of p21 in a similar manner to GppNHp (Scheidig *et al.*, 1992) and not like caged(*R*,*S*)-GTP (Schlichting *et al.*, 1990). Furthermore, it was observed that crystals of p21c′ and p21(G12)′ complexed with either caged(*R*)- or caged(*S*)-GTP are unstable and are hydrolyzed to caged P_i and GDP (Scheidig *et al.*, 1992) which was not observed for the crystals of p21c′ complexed with the diastereomer mixture caged(*R*,*S*)-GTP. Therefore, only crystals less than 2 weeks old were used for the Laue experiments.

A negative influence on crystal quality could result from the harvesting of the crystal in the artificial mother liquor enriched with DTE. To study the sensitivity of the crystals against the change of the concentration of DTE, we mounted a crystal in a flow cell and increased the concentration of DTE from approximately 5 to 100 m*M* within 5 min. The diffraction pattern before, immediately after mixing, and 10 min later showed no loss of diffraction quality.

For the previous time-resolved Laue studies on $p21^{H\text{-}ras}$, the crystals were cooled to 280 K during the photolysis to protect them from heating effects of the

powerful light flash. To examine the sensitivity of the crystals towards temperature changes, we made the following test: first exposure at 295 K, followed by cooling the crystal to 277 K within 2 min; second exposure immediately after cooling and third exposure after 30 min at 277 K. The result was that the sharp round spots of the first diffraction pattern were lost in the second exposure (streaky reflections) but reappeared in the third exposure. Therefore, the crystals were not cooled for the time-resolved experiments.

During the Laue experiments 29 crystals were tested [16 crystals of wild-type p21′ and 13 of the mutant p21(G12P)′] with the result that only one crystal of wild-type p21 was well ordered and the remaining gave streaky reflections. Nine crystals of the mutant form G12P of p21 were well ordered and the remaining gave split reflections indicating twinned crystals or crystal damage caused by the montage. The crystal structure of wild-type p21 and the p21 mutant G12P are refined to 1.35 and 1.5 Å, respectively. They are nearly identical (Franken *et al.*, 1993). The rate of the intrinsic GTPase reaction is similar in solution [k_{GTPase} (wild type) = 0.028 min^{-1} and k_{GTPase} (G12P mutant) = 0.043 min^{-1}, at 293 K (Franken *et al.*, 1993)] and the half time in the crystal is 40–45 min for both (at 293 K). Furthermore, the G12P mutant is very similar to the wild type in biochemical and kinetic behaviour, with the exception of the interaction with GAP (Franken *et al.*, 1993). Therefore, time-resolved crystallographic studies using the mutant are possible as the reaction rate is slow enough compared with the temporal resolution and the intrinsic GTP-hydrolysis reactions between mutant and wild type are comparable.

The mother liquor surrounding the crystal has two functions, first, as a reservoir of DTE and to enable diffusion of the leaving group out of the crystal; second as a temperature bath to prevent the crystal from heating. The latter is not a serious problem if two UG-11 filters (one coated with MgO) are used for photolysis. Much more serious is heating in the X-ray beam, especially at a wavelength range of 0.45–2.6 Å. After 2–3 s total exposure, the diffraction pattern deteriorated for all crystals. Since each exposure lasted 0.4–0.5 s and four exposures per time point were used, one crystal could only be used for one time step. Overall, nine new Laue data sets, two prior to and seven after photolysis, were collected.

Since a fresh crystal was used for each data set, and no crystal-alignment procedure was attempted, the crystal orientations were not identical for the different time points. Therefore, the difference-Fourier technique *DIFFLAUE* developed for Laue studies (Hajdu *et al.*, 1987) working with difference electron-density maps could not be used to analyze the structural changes between the different data sets. Therefore, the structure of each time point was refined independently using the coordinates of the high-resolution structure of p21c′:GppNHp (Pai *et al.*, 1990) and omitting the parts of the protein which are thought to participate in the GTPase reaction (residues 30–38 and 60–65), the nucleotide and water molecules. The refinement was limited by a number of problems: lack of high-resolution data, low percentage of completeness especially in the low-resolution range (see Table 1 and Fig. 2), accuracy of intensity determination of individual reflections and lack of homogeneity. The latter is produced by the fact that the crystal structure analysis is a three-dimensional image with an average in time and space within the diffracting volume. There are special gradients in the sample caused by the triggering mechanism (*e.g.* gradient of light intensity due to absorption) and time gradients caused by the duration of the triggering, by non-synchronicity of the reacting molecules (Boltzman distribution), and by the infinite data-acquisition time. The result of these limitations are electron-density maps which are noisier than those of monochromatic structures and which are frequently broken in the main-chain tracing even for the very stable β-sheet strands. Similar problems were discussed in the case of binding studies of human carbonic anhydrase II (Lindahl, Liljas, Habash, Harrop & Helliwell, 1992).

The interpretation of the electron-density maps in these regions was only possible by using the high-resolution monochromatic structures as a guide. Questionable parts were refined as poly-Gly chains to test whether the calculated electron-density map was model biased. In the very flexible parts it was hard or even impossible to decide whether a peak in the electron-density map is an indication for a

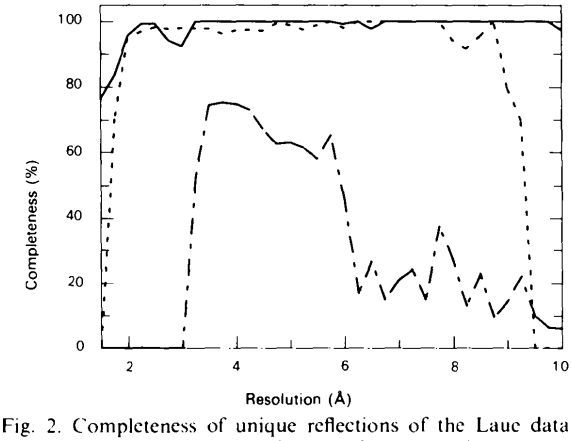

Fig. 2. Completeness of unique reflections of the Laue data set collected 2 min after initiation of the reaction (–·–) in comparison with the monochromatic data sets of p21(G12P)′:GppNHp (–; Franken *et al.*, 1993) and p21c′: caged(*R*)-GTP (---; Scheidig *et al.*, 1992).

further true conformation, a water molecule or just high noise. The deconvolution of the different conformations is very difficult. Therefore, the interpretation of the structures and the discussion is limited to regions which are well defined. Uncertain parts were omitted from the model.

In the structure of p21c′:GppNHp (Pai *et al.*, 1990) it was observed that the *B* factors of the α-, β- and γ-phosphate groups have similar values within a small range (9–12 Å^2). Decreasing electron density can be explained by an increasing *B* factor (higher mobility) or a decreasing occupancy. Therefore, the occupancy of the γ-phosphate group was determined by refining the *B* factors with occupancy values between 1.0 and 0.0. The occupancy was set to a value for which the *B* factors of the phosphate part were at the same level. The occupancy values are listed in Table 2. The decreasing percentage of occupancy is in agreement with reduced electron density at a given contour level (see Fig. 3). They are a very good indicator for the successful time-resolved monitoring of the intrinsic GTPase reaction in the crystal.

A further obvious conformational rearrangement concerns the cage group and the side chain of Tyr32 of the neighbouring molecule. The monochromatic crystal structure analysis of p21c′:caged(*R*)-GTP indicated a different orientation of Tyr32 from that seen in p21c′:GppNHp (Scheidig *et al.*, 1992) as the side chain of Tyr32 interferes sterically with the cage group of the neighbouring molecule. This was also observed in the Laue structure prior to the initiation [0 min, p21(G12P′):caged-GppNHp]. In the data set 2–4 min after photolytic removal of the cage group the side chain of Tyr32 is shifted towards the orientation observed in p21c′:GppNHp (Fig. 4). In addition, the residues 61, 62 and 63 of loop *L*4 are well defined in one conformation (Fig. 5). In the monochromatic structures of p21, the density of this loop is diffuse or can be interpreted by a superposition of different conformations (Pai *et al.*, 1990; Krengel *et al.*, 1990).

Overall, we do not have structural evidence for a conformational rearrangement prior to the GTP cleavage by p21$^{H\text{-}ras}$ (intrinsic hydrolysis reaction) as was suggested by fluorescence studies (Neal, Eccleston & Webb, 1990). One reason for this might be that caged GTP is already bound to the activated form of p21. The binding mode of the GTP part of caged GTP is nearly identical to that of GppNHp (Pai *et al.*, 1990) and no significant shift is seen in the Laue structure 2–4 min after photolytical removal of the cage group. Because of the low resolution and incompleteness of the data sets no water molecules were incorporated into the structure. However, no electron-density peak at the position of the activated water molecule WAT175 (Pai *et al.*, 1990) could be detected. In the Laue structure 2–4 min after photolysis, the residues Gln61, Glu62 and Glu63 of the 'catalytic' loop *L*4 are very well defined and show a new, so far unknown, conformation. In this conformation Gln61 is very close to the γ-phosphate group (approximately 3.3 Å) in an orientation which is close to that proposed by Privé *et al.* (1992). Furthermore, at the end of the reaction (data set corresponding to 90–92 min after photolysis) the side chain of Asp57 comes very close to the Mg^{2+} ion. In the monochromatic structure of p21c′:GDP derived from p21c′:caged(*R,S*)-GTP 24 h after photolysis (Schlichting *et al.*, 1990) the side chain of Asp57 makes a direct coordination of the Mg^{2+} ion. We propose that the water molecule WAT173 [ligand of Mg^{2+} in p21c′:GppNHp (Pai *et al.*, 1990)] is directly involved in the hydrolysis reaction (but not necessarily as the attacking water) and is removed together with the leaving inorganic phosphate group. In the monochromatic structures of p21c′:GDP there is a water molecule between the Mg^{2+} ion and the side chain of Asp57 (Tong, de Vos, Milburn & Kim, 1991). Therefore, it seems that the coordination sphere with this water molecule is more stable but might be established with a very slow rate, possibly during an Mg^{2+} exchange with the surrounding solution.

The main trigger for larger conformational rearrangements due to the hydrolysis reaction seems to be the loss of the hydrogen bond between the main-chain Thr35 NH and the γ-phosphate group. As soon as this interaction is too weak or lost, a complete rearrangement of the so-called effector loop *L*2 occurs [seen in monochromatic structures of p21c′:caged(*R*)-GTP, p21(Y32W)′:caged(*R*)-GTP and p21(G12P)′:C3-GTP which will be published elsewhere]. No change in the orientation of the helix α2 could be seen as proposed by Stouten, Sander, Wittinghofer & Valencia (1993). The analysis of the crystal packing indicates that such a conformational change is not compatible with the stability of the crystal lattice (data not shown).

Concluding remarks

Time-resolved investigations of p21$^{H\text{-}ras}$ were extended by using the 1:1 complex between the mutant p21(G12P)′ and a pure diastereomer, either the *R* or *S* isomer at the asymmetrically substituted C atom in the cage group of P^3-1-(2-nitrophenyl)-ethylguanosinetriphosphate together with a modified crystallization protocol. The refinement of the data showed that it is possible to observe reactions occurring in the crystal. Presently, the structural interpretation is limited to small changes reflecting two discrete states, meaning that the residue or group in question has only two well defined conformations.

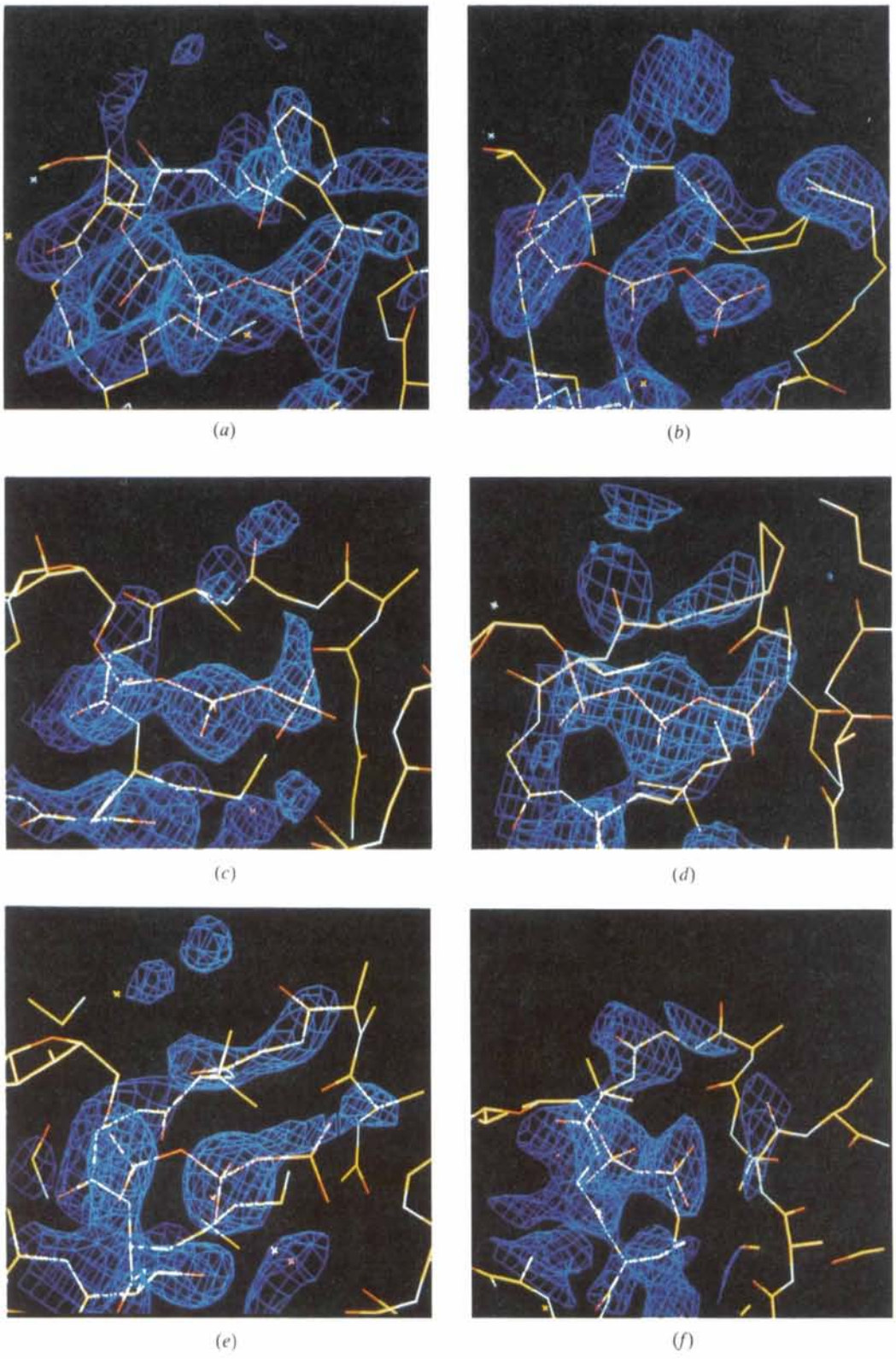

Fig. 3. Active site of p21 at different time points of the intrinsic GTPase reaction. The protein and nucleotide atoms are given in different colors. The cut off of the $(2F_o - F_c)$ electron-density maps is 25% of the maximum. (*a*) $t = 0$ min, p21(G12P)′:caged(*R*,*S*)-GppNHp; (*b*) $t = 2$ min, p21(G12P)′:GTP; (*c*) $t = 11$ min, p21(G12P)′:GTP/GDP; (*d*) $t = 20$ min, p21(G12P)′:GTP/GDP; (*e*) $t = 30$ min, p21(G12P)′:GTP/GDP; (*f*) $t = 90$ min, p21(G12P)′:GDP.

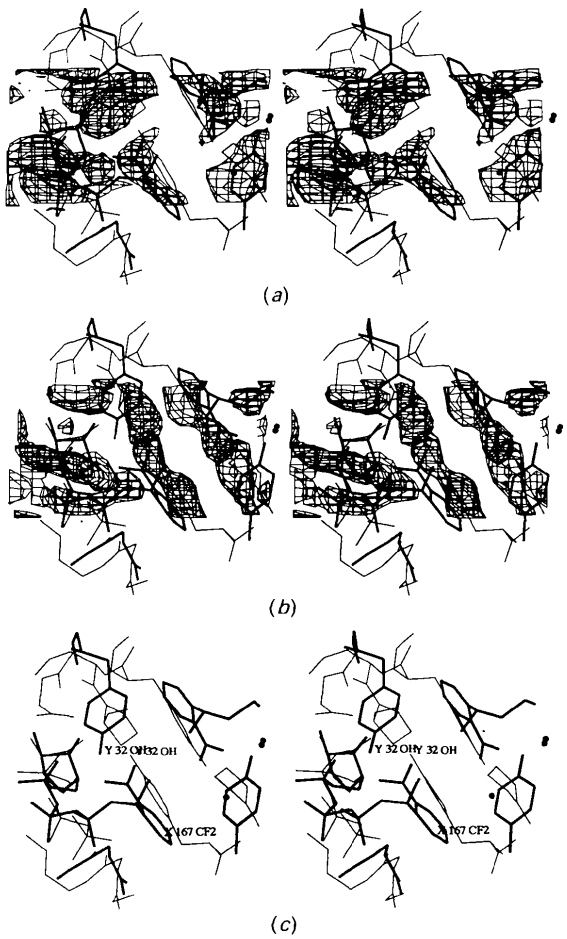

Fig. 4. Crystal-packing interactions concerning the residue Tyr32 and the cage group. The view is along the crystallographic twofold axis. The cut off of the $(2F_o - F_c)$ electron-density maps is 25% of the maximum. (*a*) $t = 0$ min, p21(G12P)′:caged(*R*,*S*)-GppNHp (thick lines, with electron density) superimposed with the structure $t = 2$ min, p21(G12P)′:GTP (thin lines); (*b*) $t = 2$ min, p21(G12P)′:GTP $t = 2$ min (thick lines, with electron density) superimposed with the structure $t = 0$ min, p21(G12P)′caged(*R*,*S*)-GppNHp (thin lines); (*c*) both structures superimposed without electron density.

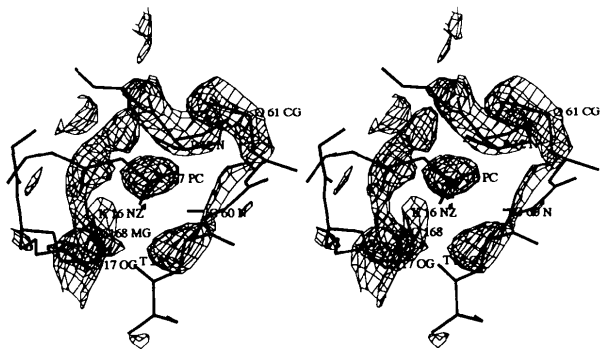

Fig. 5. Final $(2F_o - F_c)$ electron-density map, in stereo, around the γ-phosphate group of the Laue structure 2 min after initiation of the reaction including the residues Thr58 to Gln61 of the loop *L*4. The electron density is contoured at the level of 25% cut off.

The incompleteness and the lack of high-resolution data as observed in our studies is not necessarily due to the Laue method itself, since other groups were able to collect very good data with a high percentage of completeness (Bartunik, Bartsch & Qichen, 1992; Singer *et al.*, 1992). Our problems originate mainly from the special experimental situation we have: no prealignment of the crystal, only three to four different orientations per data set, use of fibres and surrounding mother liquor which produce shadowing, diffuse scattering and, therefore, a significant high background level, and use of a very broad wavelength range. Furthermore, we could not use unscrambling of the wavelength harmonic overlaps due to very high *R* factors of the terms obtained. Because of the duration of triggering (10 flashes within 90 s) and collecting four diffraction patterns (90 s overall, 0.5 s exposure^{-1} and 25 s turn^{-1} of the film carousel; the actual temporal resolution is between 2 and 4 min), additional effects such as heating of the crystal by the X-ray beam and temporal and spatial inhomogeneities in the volume of the diffracting crystal will obscure the result further. Therefore, the calculated electron-density distribution will describe an average of different structures rather than only one structure. Nevertheless, keeping these limiting factors in mind, p21 is a very good system to study a protein reaction in the crystal using time-resolved X-ray crystallography. This is the case, because the half time of the GTPase reaction in the crystal (40–50 min at 293 K) is much longer than the time uncertainty. Furthermore, the photolytic removal of the cage group is very efficient and the kinetic behaviour in the crystal is very reproducible.

Three conformational rearrangements could be detected in the crystals of the mutant form G12P of truncated p21 (residues 1–166) by the present time-resolved X-ray crystallographic study after photolysis of the cage group. In the first data set, 2–4 min after the reaction initiation, Tyr32 is shifted towards the orientation where it is found in the p21c′:GppNHp structure (Pai *et al.*, 1990). Gln61 is found in a conformation where the carbamoyl group of the side chain is close to the γ-phosphate group and the whole loop region from 58 to 61 is wrapped around that γ-phosphate. These orientations were not observed or detectable in the monochromatic studies of wild-type p21 or in the data sets with a longer time gap between photolysis and exposure. For the data sets corresponding to 11–13, 20–22 and 30–32 min this is due to the very diffuse and broken electron density in the respective regions. In the data set for 90–92 min after initiation, where the reaction was approximately 90% finished, electron density for a new orientation of the loop region Tyr32 to Ile36 is visible which is comparable to the conformation determined by monochromatic X-ray structure

analysis using the caged GTP/photolysis/24 h hydrolysis approach (Schlichting *et al.*, 1990). The electron density for the γ-phosphate group decreased from the first data set to the last data set where no more density was found at the appropriate position. In the data sets for 11–13, 20–22 and 30–32 min, the loop regions *L*2 (residues 32–36) and *L*4 (residues 61–65) revealed very diffuse electron density. This is an indication of the absence of a transiently stable intermediate in the intrinsic GTP-hydrolysis reaction. As caged GTP in our crystals has a binding mode nearly identical to that of GppNHp or GTP, we cannot get any hints regarding a conformational rearrangement prior to the GTP cleavage as proposed by Neal *et al.* (1990). Therefore, our conclusion for the intrinsic GTPase reaction is that the rearrangement of the loop region *L*2 and probably of the loop region *L*4 is the result of the loss of the γ-phosphate group. There are two main interactions, one of Gly60 N and one of Thr35 N with the γ-phosphate group. In particular, as soon as Thr35 is no longer attached to the γ-phosphate, loop L2 is in a non-stable orientation and is rearranged to reach a more stable conformation.

The results of our experiments can be interpreted such that structural information at the atomic level is available if the short-lived intermediates are transiently accumulated in the crystal, which seems not to be the case for the intrinsic GTPase reaction of p21(G12P)$^{H\text{-}ras}$. Larger rearrangements resulting in more than one intermediate conformation produce diffuse and broken electron density which we were not able to deconvolute. This last limitation is not a problem of the Laue method exclusively, since the incorporation of alternative conformations is a problem in monochromatic structure determination also. Our experiments and results suggest that especially larger rearrangements and intermediates which are not transiently stable are not easily detectable and description is limited to the qualitative level.

Special thanks are due to J. Habash, J. R. Helliwell, C. Nave, K. Poole, G. Rapp, I. Schlichting, V. Stoll and A. W. Thompson for their help in data collection and data processing. We thank the staff of Daresbury Laboratory for the excellent facilities and service at the storage ring. Financial support by the Fonds der Chemischen Industrie and the Deutsche Forschungsgemeinschaft is gratefully acknowledged. We would like to thank Wolfgang Kabsch for crystallographic advice and Kenneth C. Holmes for continuous support.

References

Amoros, J. L., Buerger, M. & Amoros, M. C. (1975). *The Laue Method*. New York: Academic Press.

Barbacid, M. (1987). *Annu. Rev. Biochem.* **56**, 779–827.

Bartunik, H. D., Bartsch, H. H. & Qichen, H. (1992). *Acta Cryst.* A**48**, 180–188.

Bollag, G. & McCormick, F. (1991). *Nature (London)*, **351**, 576–579.

Brammer, R. C., Helliwell, J. R., Lamb, W., Liljas, A., Moore, P. R., Thompson, A. W. & Rathbone, K. A. (1988). *Nucl. Instrum. Methods A*, **271**, 678–687.

Brünger, A. T. (1988). *J. Mol. Biol.* **203**, 803–816.

Brünger, A. T., Kuriyan, J. & Karplus, M. (1987). *Science*, **235**, 458–460.

Cambillau, C. (1989). In *Silicon Graphics Geometry Partner Directory*, Spring Volume. Silicon Graphics, Mountain View, CA, USA.

Cruickshank, D. W. J., Carr, P. D. & Harding, M. M. (1992). *J. Appl. Cryst.* **25**, 285–293.

Franken, S. M., Scheidig, A. J., Krengel, U., Rensland, H., Lautwein, A., Scheffzek, K., Geyer, M., Goody, R. S., Kalbitzer, H.-R., Pai, E. F. & Wittinghofer, A. (1993). *Biochemistry*. In the press.

Friedrich, W., Knipping, P. & Laue, M. (1912). *Sitzungsber. K. Akad. Wiss.* pp. 303–322.

Hajdu, J. & Andersson, I. (1993). *Annu. Rev. Biophys. Biomol. Struct.* **22**, 467–498.

Hajdu, J. & Johnson, L. N. (1990). *Biochemistry*, **29**, 1669–1678.

Hajdu, J., Machin, P. A., Campbell, J. W., Greenhough, T. J., Clifton, I. J., Zurek, S., Gover, S., Johnson, L. N. & Elder, M. (1987). *Nature (London)*, **329**, 178–181.

Helliwell, J. R., Habash, J., Cruickshank, D. W. J., Harding, M. M., Greenough, T. J., Campbell, J. W., Clifton, I. J., Elder, M., Machin, P. A., Papiz, M. Z. & Zurek, S. (1989). *J. Appl. Cryst.* **22**, 483–497.

Jurnak, F., Heffron, S. & Bergmann, E. (1990). *Cell*, **60**, 525–528.

Krengel, U., Schlichting, I., Scherer, A., Schumann, R., Frech, M., John, J., Kabsch, W., Pai, E. F. & Wittinghofer, A. (1990). *Cell*, **62**, 539–548.

Lindahl, M., Liljas, A., Habash, J., Harrop, S. & Helliwell, J. R. (1992). *Acta Cryst.* B**48**, 281–285.

McCormick, F. (1989). *Cell*, **56**, 5–8.

McCray, J. A. & Trentham, D. R. (1989). *Annu. Rev. Biophys. Chem.* **18**, 239–270.

Milburn, M. V., Tong, L., DeVos, A. M., Brünger, A., Yamaizumi, Z., Nishimura, S. & Kim, S.-G. (1990). *Science*, **247**, 939–945.

Moffat, J. K. (1989). *Annu. Rev. Biophys. Biophys. Chem.* **18**, 309–332.

Neal, S. E., Eccleston, J. F. & Webb, M. R. (1990). *Proc. Natl Acad. Sci. USA*, **87**, 3562–3565.

Pai, E. F., Krengel, U., Petsko, G. A., Goody, R. S., Kabsch, W. & Wittinghofer, A. (1990). *EMBO J.* **9**, 2351–2359.

Privé, G. G., Milburn, M. V., Tong, L., de Vos, A. M., Yamaizumi, Z., Nishimura, S. & Kim, S.-H. (1992). *Proc. Natl Acad. Sci. USA*, **89**, 3649–3653.

Rapp, G. & Güth, K. (1988). *Pfluegers Arch.* **411**, 200–203.

Read, R. J. (1986). *Acta Cryst.* A**42**, 140–149.

Scheidig, A., Pai, E. F., Schlichting, I., Corrie, J. E. T., Reid, G. P., Wittinghofer, A. & Goody, R. S. (1992). *Philos. Trans. R. Soc. London Ser. A*, **340**, 263–272.

Schlichting, I., Almo, S. C., Rapp, G., Wilson, K., Petratos, K., Lentfer, A., Wittinghofer, A., Kabsch, W., Pai, E. F., Petsko, G. A. & Goody, R. S. (1990). *Nature (London)*, **345**, 309–315.

Schlichting, I., Rapp, G., John, J., Wittinghofer, A., Pai, E. F. & Goody, R. S. (1989). *Proc. Natl Acad. Sci. USA*, **86**, 7687–7690.

Singer, P. T., Carty, R. P., Berman, L. E., Schlichting, I., Stock, A., Samalas, A., Cai, Z., Mangel, W. F., Jones, K. W. & Sweet, R. M. (1992). *Philos. Trans. R. Soc. London Ser. A*, **340**, 285–300.

Stouten, P. F. W., Sander, Chr, Wittinghofer, A. & Valencia, A. (1993). *FEBS Lett.* **320**, 1–6.

Tong, L., de Vos, A. M., Milburn, M. V. & Kim, S.-H. (1991). *J. Mol. Biol.* **217**, 503–517.